

A mutation causing short snout and lens spots that maps to Chromosome 4

Michelle M. Curtain, Coleen Kane, Leah Rae Donahue, Ph.D.

Source of Support: This research was supported by NIH grants EY015073-05Z and OD010972 to Leah Rae Donahue

Mutation (allele) symbol: *shsn*

Mutation (allele) name: short snout

Strain of origin: B6.129P2-*Apoe*^{*tm1Unc*}/J

Current strain name: B6(129P2)-*shsn*/GrsrJ

Stock #008753 (jaxmice.jax.org)

Phenotype categories: craniofacial, eyes

Origin and Description

A mutation that causes a shortened, squared snout arose spontaneously in the B6.129P2-*Apoe*^{*tm1Unc*}/J colony (Stock #002052) at The Jackson Laboratory and was named short snout, *shsn*. The *Apoe*^{*tm1Unc*} mutation was bred out of the mutant subline without altering the short snout phenotype. Mutants are viable and fertile, and the colony is maintained by mating a heterozygote of either gender to a homozygous sibling.



A 10-week-old *shsn* mutant is on the left and control littermate on the right.

Genetic analysis

That *shsn* is inherited as an autosomal recessive mutation was proven by mating a mutant to a C57BL/6J. There were no affected mice in the F1 generation but there were affected mice in the F2 population. No sex linkage was found.

Following our standard mapping protocol a mutant from the colony was mated to a CAST/EiJ and F1 obligate heterozygotes were intercrossed. Samples from 40 mutant and 78 unaffected siblings were submitted to the Fine Mapping Laboratory at The Jackson Laboratory for SNP analysis. *shsn* mapped to Chromosome 4 between *D4Mit111* at 53.5 Mb and *D4Mit87* at 62 Mb. Whole exome sequencing¹ did not reveal any mismatched alleles unique to the *shsn*

mutation so the causative gene remains unknown.

Biological characterization

Craniofacial morphology of twelve-week-old mice

Skulls were prepared by incomplete maceration in potassium hydroxide, stained with alizarin red, and stored in undiluted glycerin (Green, 1952). Morphological measurements of the skull (Table 1 – see protocol¹) were made using digital calipers (Stoelting, Wood Dale, IL) with previously established landmarks (Richtsmeier, 2000, see protocol¹). Skull, nose and lower jaw lengths, and skull height, were all significantly affected. Jaw length ratio, skull to nose length ratio, skull height to length ratio, skull length to width ratio, skull height to width ratio differences were significant between the sexes and/or genotypes. (graphs 2, 3, 4).

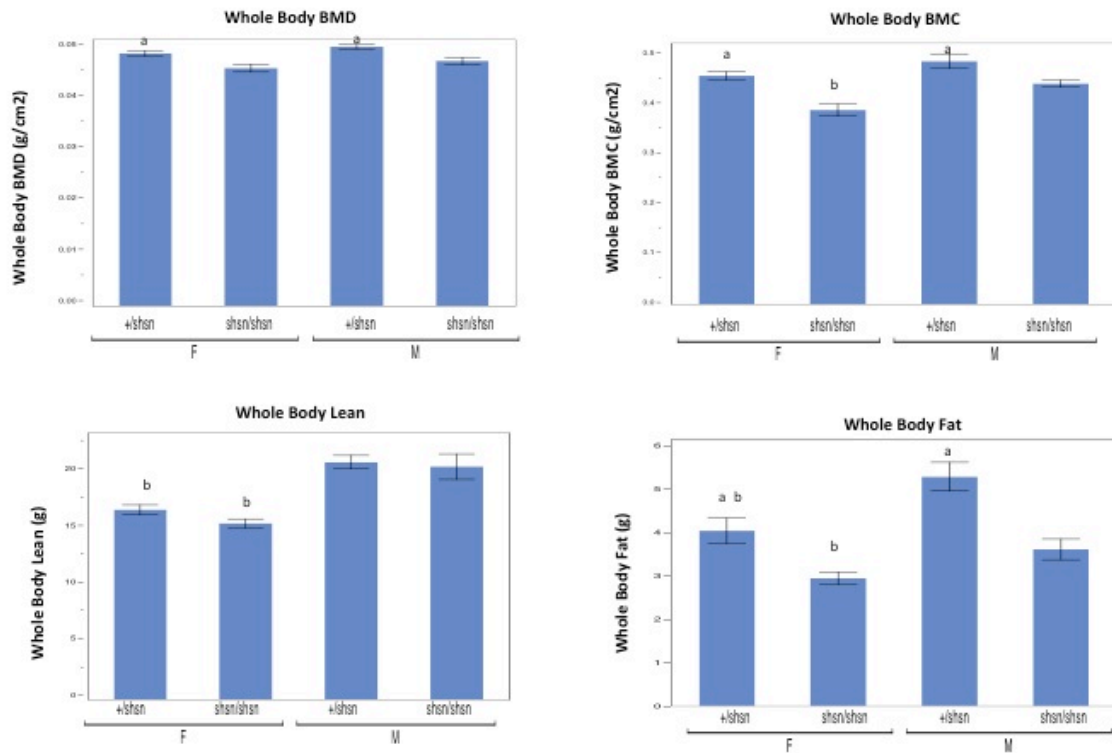
Table 1: Measurements and Calculated Ratios of Twelve-week-old B6;129P2-*shsn*/J skulls stained with Alizarin Red (n=6; mean± SEM; ^{ab}p≤ 0.05)

Measurements	Male +/ <i>shsn</i>	Male <i>shsn/shsn</i>	Female +/ <i>shsn</i>	Female <i>shsn/shsn</i>
Skull Length	22.64± 0.195 ^a	19.91± 0.355	22.08± 0.430 ^a	19.62± 0.272
Nose Length	15.79± 0.083 ^a	13.40± 0.237	15.75± 0.255 ^a	12.99± 0.247
Skull Height	10.66± 0.142 ^a	9.88 0.196 ^b	10.07± 0.343	10.87± 0.112
Skull Width	10.78± 0.078	10.52± 0.171	10.37± 0.233	10.62± 0.096
Inner Canthal Distance	5.81± 0.153	5.59± 0.191	5.83± 0.404	5.62± 0.154
Lower Jaw Length	11.40± 0.124 ^{ab}	10.42± 0.308	10.79± 0.157	10.29± 0.241
Upper Jaw Length	15.60± 0.191	13.80± 0.316	15.54± 0.307	13.52± 0.221
Jaw Length Ratio	1.36± 0.024 ^b	1.33± 0.019	1.44± 0.0167 ^a	1.33± 0.020
Skull/Nose Length Ratio	1.43± 0.014 ^a	1.49± 0.012	1.40± 0.015 ^a	1.51± 0.030
Skull Height/Length Ratio	0.47± 0.005	0.50± 0.011 ^b	0.46± 0.115 ^a	0.55± 0.010
Skull Length/Width Ratio	2.10± 0.021 ^a	1.90± 0.034	2.13± 0.017 ^a	1.85± 0.028
Skull Height/Width Ratio	0.99± 0.016 ^a	0.94± 0.005 ^b	0.97± 0.023 ^a	1.03± 0.009

Graph 1

12 Week B6;129P2-*shsn*/J
split by sex and genotype (n=6; mean± SEM p< 0.05)

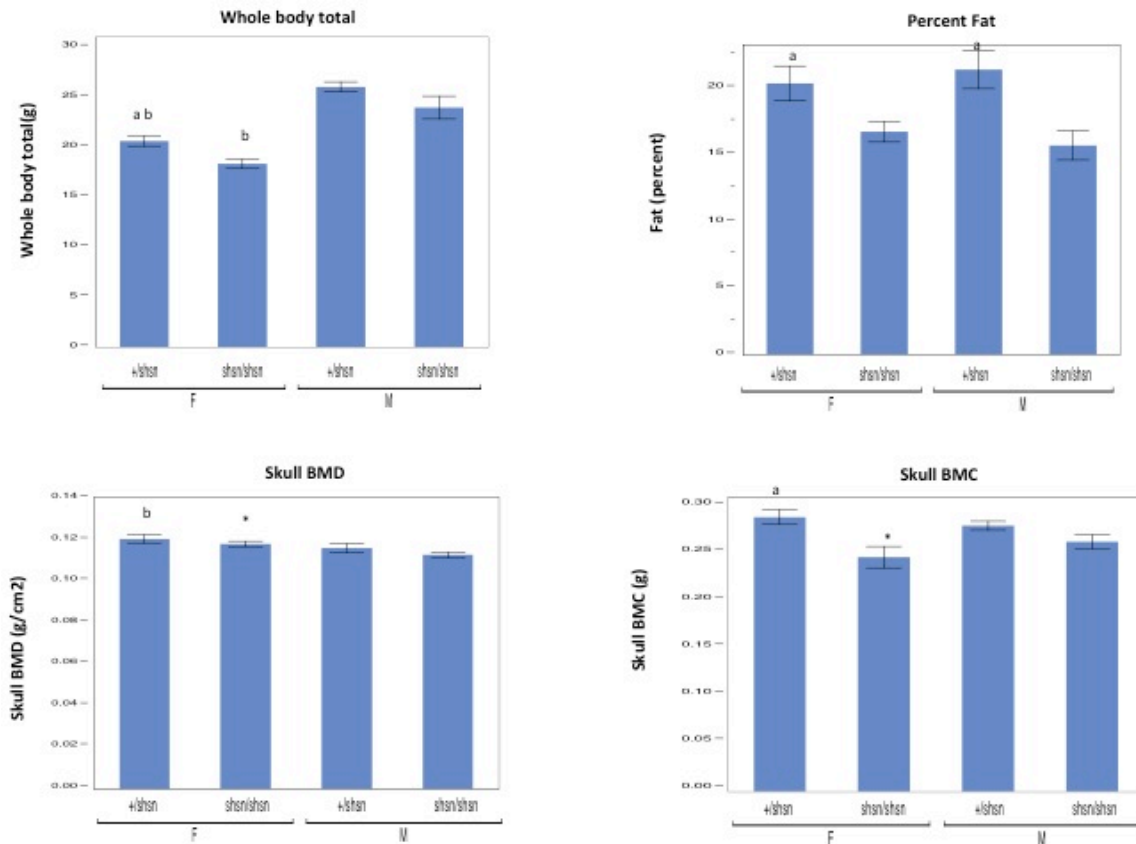
Significant differences
a +/-*shsn* vs. +/+ within sex
b male vs. female within genotype



Graph 2

12 Week B6;129P2-*shsn*/J
split by sex and genotype (n=6; mean± SEM p< 0.05)
* n=5

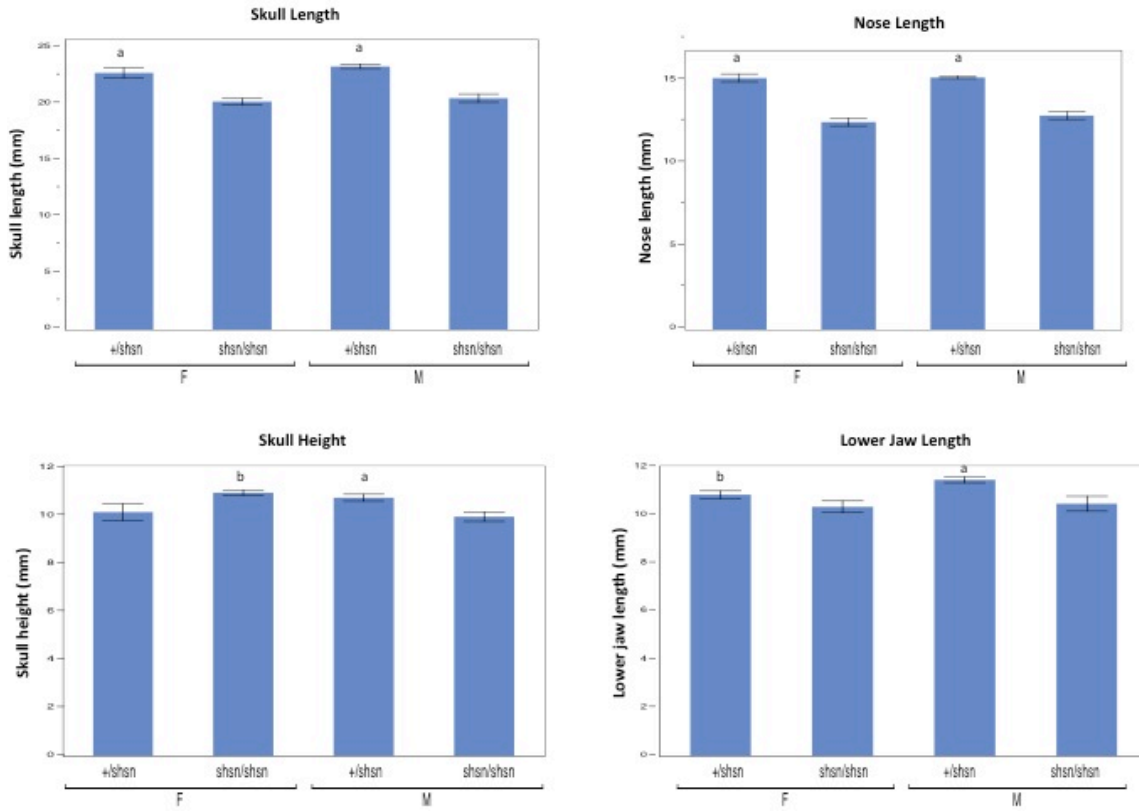
Significant differences
a +/-*shsn* vs. +/+ within sex
b male vs. female within genotype



Graph 3

12 Week B6;129P2-*shsn*/J
split by sex and genotype (n=6; mean±SEM p≤ 0.05)

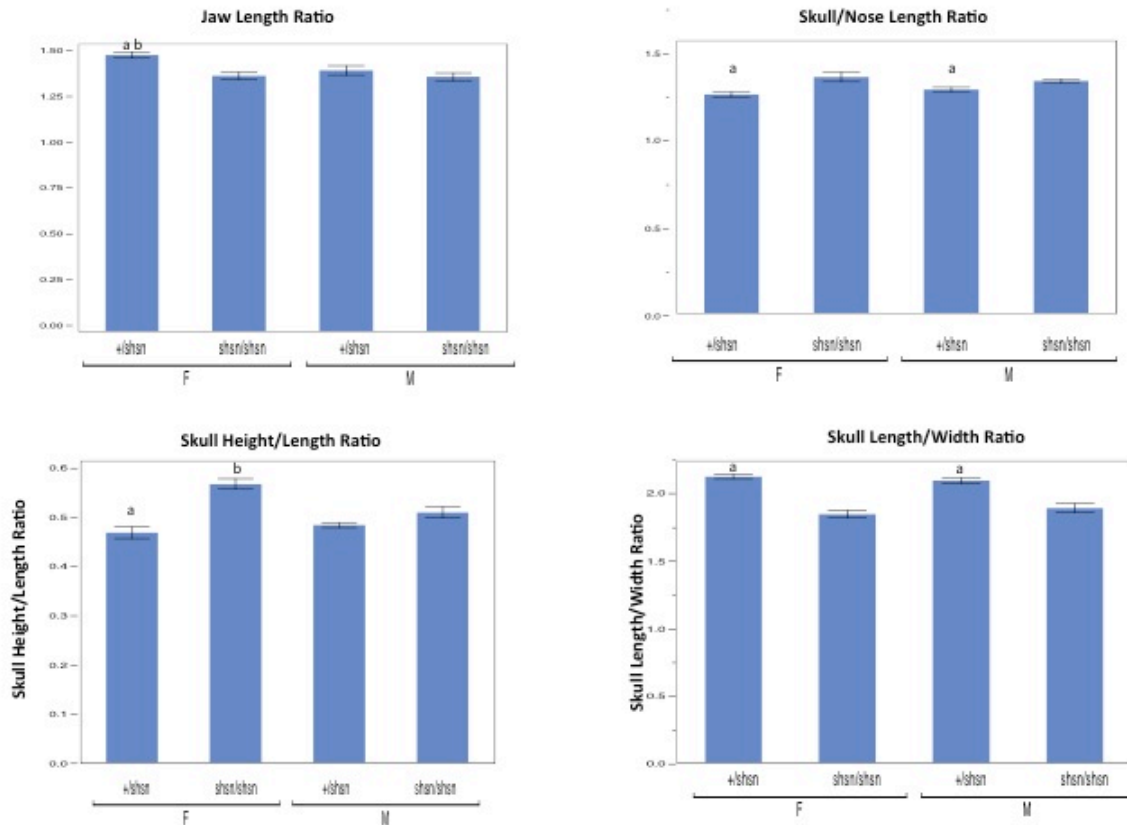
Significant differences
a +/*shsn* vs. +/+ within sex
b male vs. female within genotype



Graph 4

12 Week B6;129P2-*shsn*/J
split by sex and genotype (n=6; mean±SEM p≤ 0.05)

Significant differences
a +/*shsn* vs. +/+ within sex
b male vs. female within genotype



DEXA analysis of whole body aBMD and body composition of twelve-week-old mice

Whole body, areal bone mineral density (aBMD), bone mineral content (BMC) and body composition (lean, fat and % fat mass) were assessed by PIXImus densitometry (GE LUNAR, Madison, WI) (Table 2- see protocol¹). Whole body BMD, whole body BMC, whole body lean, whole body fat, percent fat, skull BMD, skull BMC, skull BMD to body BMD ratio, and total weight were all significantly affected between the sexes and/or genotypes (graphs 1 and 2 above).

Table 2: PIXImus Densitometric Measurements of
Twelve-week-old B6;129P2-*shsn*/J
(n=6; mean± SEM; ^ab_p≤ 0.05)

Measurements	Male +/ <i>shsn</i>	Male <i>shsn/shsn</i>	Female +/ <i>shsn</i>	Female <i>shsn/shsn</i>
Whole Body BMD (g/cm ²)	0.486± 0.00045 ^a	0.459± 0.00065	0.0473± 0.00051 ^a	0.0446± 0.0007
Whole Body BMC (g)	0.465± 0.0341 ^a	0.422± 0.0066 ^b	0.437± 0.0077 ^a	0.371± 0.0117
Whole Body Lean (g)	20.0± 0.57 ^b	19.6± 1.07 ^b	16.0± 0.41	14.8± 0.38
Whole Body Fat (g)	5.2± 0.47 ^{ab}	3.5± 0.23 ^b	3.9± 0.28 ^a	2.9± 0.14
Total Mass (g)	25.2± 0.46 ^b	23.1± 1.10 ^b	19.9± 0.49 ^a	17.7± 0.43
% Fat	21 ^a	15	20 ^a	16
Skull BMD (g/cm ²)	0.1172± 0.00133 ^b	0.1121± 0.00130	0.1197± 0.00200	0.1153± 0.00210 [*]
Skull BMC (g)	0.270± 0.0045	0.254± 0.0070	0.279± 0.0073 ^a	0.238± 0.0109 [*]
Skull BMD/Body BMD	2.415± 0.0349 ^b	2.442± 0.0345 ^b	2.530± 0.0329	2.594± 0.0311 [*]

*n=5

Pathology

No additional abnormalities were detected in a routine pathological screening of one homozygous male and one heterozygous male both at eleven weeks of age.

An ophthalmoscope was used to view the eyes of mutants and littermate controls ranging from one to three months of age. The retinas were normal but 15 out of 16 homozygotes had lens spots and photosensitivity; eight heterozygous littermates had no lens spots.

Hearing was assessed by auditory brainstem response testing (ABR)². In testing of subjects ranging from one to three months of age, three out of five mutants had profound hearing loss while the two other mutants and four controls had normal hearing. There may be a hearing loss phenotype segregating in this B6;129P2 genetic background, but this hearing loss does not appear to be attributable to the *shsn* mutation.

Discussion

The *shsn* mutation not only shortens the face but the whole body is affected with lower bone mineral density and content along with reduced size, lean and fat in mutants.

Acknowledgements

For their expertise and assistance, we wish to acknowledge:

Pathological evaluation: Roderick T. Bronson, PhD

Hearing assessment: Chantal Longo-Guess

Evaluation of the eyes: Bo Chang, MD and Ron E. Hurd

Whole exome sequence analysis: Heather E. Fairfield

Discovery of the mutation: Melanie Atherton

Editing and web posting: Aimée Picard

Protocols

¹Standard Protocols and Procedures of The Jackson Laboratory Craniofacial Mutant Resource:

Mouse Colony Maintenance

Craniofacial Resource mice are housed in 51 square inch polycarbonate boxes, on bedding composed of sterilized shavings of Northern White Pine, under 14:10 hour light:dark cycles. A diet of autoclaved NIH 31 (6% fat diet, Ca:P of 1.15:0.85, 19% protein, vitamin and mineral fortified; Purina Mills International, Richmond, IN) and water acidified with HCl to achieve a pH of 2.8-3.2 (which prevents bacterial growth) are freely available. Mouse colony maintenance and use is reviewed and approved by The Jackson Laboratory Institutional Animal Care and Use Committee and is in accordance with The National Institutes of Health guidelines for the care and use of animals in research.

PIXImus Densitometry

PIXImus scans (PIXImus, LUNAR, Madison, WI) which provide skeletal and body composition data such as Bone Mineral Density (BMD, g/cm²), Bone Mineral Content (BMC, g), body mass (g), lean mass (g), fat mass (g), and % fat mass, are completed on groups of 6 male and 6 female 12 week old mutant and control mice. The skulls and bodies are scanned separately to provide independent data on skull BMD and BMC and body BMD and BMC. The PIXImus small animal densitometer (DEXA) has a resolution of 0.18 x 0.18 mm pixels and is equipped with software version 1.46. The PIXImus is calibrated routinely with a phantom utilizing known values, and a quality assurance test is performed daily. The variability in precision for measuring total body BMD is, less than 1%, and approximately 1.5% for specialized regions such as the skull. The correlation between PIXImus BMD measurements of 614 lumbar vertebrae compared to peripheral quantitative computerized tomography (pQCT) measurements was found to be significant ($p < 0.001$; $r = 0.704$) (Donahue, 1999).

Faxitron X-rays

X-rays at 5X magnification of the skull and at 3X magnification of the body of a male and female mutant and control at 12 weeks of age are obtained using a Faxitron MX20 cabinet X-ray (Faxitron X-Ray Corp., Wheeling, IL, USA) and Kodak Min-R 2000 mammography film (Eastman Kodak Co., Windsor, CO, USA). X-rays are then analyzed to determine the specificity of the skeletal phenotype.

Skull Preparation

Skulls of 6 male and 6 female mutants and controls are collected at 12 weeks of age, prepared by incomplete maceration in potassium hydroxide, stained with alizarin red, and stored in undiluted glycerin (Green, 1952). During the collection process, right ear pinnae are measured with digital hand calipers (Stoelting, Wood Dale, IL, USA).

Hand Caliper Skull Measurements

Seven measurements taken with hand held digital calipers are used routinely to define skull morphology at the Lab's craniofacial resource. These measures have a high degree of accuracy and precision in our hands and are able to discriminate differences between mutant and control skull characteristics. Our linear measures have been added to those illustrated by Dr. Joan Richtsmeier in her paper characterizing craniofacial differences in mouse models of Down Syndrome using three dimensional anatomical landmarks (Richtsmeier, 2000. Dev. Dyn. Feb; 217(2):137-45). Skulls are cleared with potassium hydroxide and stained with alizarin red dye in preparation for caliper measurements to be taken.

Skeletal Preps

In many cases whole skeletons of mutant and control mice are cleared in 1% KOH, stained with alizarin, stored in glycerin (Green, 1952) and then evaluated for skeletal malformations. Malformations found can indicate that the craniofacial phenotype is part of a greater syndrome.

Data Analysis

Hand caliper skull measurements and PIXImus skeletal and body composition data are evaluated using StatView 4.5 software (Abacus Cary, NC) for Macintosh computers. Differences are considered significant when $p < 0.05$.

Molecular Mapping

Mutations resulting in unique phenotypes are genetically mapped to establish the chromosomal location of the causative gene. In the past, the Craniofacial Mutant Resource relied on high-resolution mapping to narrow the

genetic interval to a manageable size for candidate gene analysis. With the advent of sequence capture and high throughput sequencing (HTPS) techniques, this level of resolution is no longer required. Genetic mapping to rough chromosomal position still provides a number of useful advantages however, such as a reduced computational burden, fewer variants to validate, and greater confidence in variant causality. To identify causative mutations we use a combination of genetic mapping and HTPS. We have found that mapping a gene at least to a chromosome greatly facilitates the analyses of HTPS. Our studies use a combination of 1-10 Mb interval-specific, gene-specific, and whole exome approaches to identify a wide spectrum of mutation types across diverse genetic backgrounds.

Sequencing

Exome capture and sequencing

Once linkage is established and a broad chromosomal location identified, we employ whole exome capture and HTPS to identify potential causative variants. Whole DNA exomes from mutant samples are captured using an in-solution, hybridization-based probe pool developed in our group in collaboration with Roche-Nimblegen. The content of the probe pool is defined by the unified mouse gene catalog which, excluding UTR sequences, olfactory receptors and pseudogenes, encompasses approximately 50 Mb of genomic sequence. Our preliminary exome data indicate high capture sensitivity and specificity, >96.7% of the targeted bases covered with just one lane of 75 bp paired-end on the Illumina GAIIX.

Our primary sequencing approach is to sequence whole exomes from enriched mutant DNA samples and to multiplex where possible (Fairfield, et al., 2011). An additional advantage of the paired end sequencing approach is that it provides positional information that is critical for the identification of spontaneous mutations that are due to genome rearrangements (larger insertions or deletions).

Analysis and validation

All raw sequence data analysis, including read mapping and SNP/mutation calling are performed by the Computational Science service at JAX, using Galaxy sequence analysis tools. Multiple candidate variations are detected in each strain, but most are eliminated upon validation. For validation, each candidate mutation is PCR amplified from up to 10 other individuals within the same mutant pedigree. Each PCR amplicon is subjected to Sanger sequencing. In the majority of the cases, non-mutagenic variants will not segregate with the phenotype, but bona fide mutations will. Validation is not attempted until sufficient sequencing coverage has been obtained, as indicated by comparison of computational analysis of parameters like '% target bases covered' and by comparison of the variant profiles obtained to the Sanger whole genome sequencing data.

References

- Donahue LR, Rosen CJ, Beamer WG. (1999) *Comparison of Bone Mineral Content and Bone Mineral Density in C57BL/6J and C3H/HeJ Female Mice by pQCR (Stratec XCT 960M) and DEXA (PIXImus)*. Thirteenth International Mouse Genome Conference. Philadelphia, PA.
- Fairfield H, Gilbert GJ, Barter M, Corrigan RR, Curtain M, Ding Y, D'Ascenzo M, Gerhardt DJ, He C, Huang W, Richmond T, Rowe L, Probst FJ, Bergstrom DE, Murray SA, Bult C, Richardson J, Kile BT, Gut I, Hager J, Sigurdsson S, Mauceli E, Di Palma F, Lindblad-Toh K, Cunningham ML, Cox TC, Justice MJ, Spector MS, Lowe SW, Albert T, Donahue LR, Jeddelloh J, Shendure J, Reinholdt LG. 2011. *Mutation discovery in mice by whole exome sequencing*. *Genome Biology* 12: R86.
- Green, MC. (1952) *A rapid method for clearing and staining specimens for the demonstration of bone*. *The Ohio Journal of Science* 52(1):31-33. January 1952.
- Manly KF, Cudmore RH, Jr., Meer JM. (2001) *Map Manager QTX, cross-platform software for genetic mapping*. *Mamm. Genome* 12:930-932.
- Richtsmeier JT, Baxter, LL, Reeves, RH. (2000) *Parallels of craniofacial maldevelopment in Down syndrome and Ts65Dn mice*. *Dev. Dyn.* Feb;217(2):137-45.
- Truett GE, Heeger P, Mynatt RL, Truett AA, Walker JA, Warman ML. (2000) *Preparation of PCR-quality mouse genomic DNA with hot sodium hydroxide and Tris (HoSHOT)*. *Biotechniques* 29;52-54.

² **ABR thresholds** in mice are determined using a semi-automated computer system (Intelligent Hearing Systems, Miami, Florida). Subdermal needle electrodes are inserted at the vertex and ventrolaterally to both ears of anesthetized mice. Specific auditory stimuli from 10-100 dB SPL are delivered binaurally through plastic tubes from high frequency transducers. ABR thresholds are obtained, in an acoustic chamber, for clicks and for 8, 16, and 32 kHz pure-tone pips.